CRYSTAL GROWTH & DESIGN

Article

pubs.acs.org/crystal

Intermolecular Interactions in Bromo-, Methyl-, and Cyanoimidazole Derivatives

Christopher J. Serpell*,† and Paul D. Beer

Chemistry Research Laboratory, Department of Chemistry, University of Oxford, Mansfield Road, Oxford, OX1 3TA, U.K.

Supporting Information

ABSTRACT: Materials containing bistable N−H···N hydrogen bonds, such as imidazole crystals, show promise for applications in electronics. Herein, we examine the effect of imidazole functionalization upon structural parameters relating to proton transfer, molecular rotation, and order−disorder transitions. Three different substituents are studied: methyl-, bromo-, and cyano-, resulting in steric, electronic, and supramolecular modification of the imidazole core.

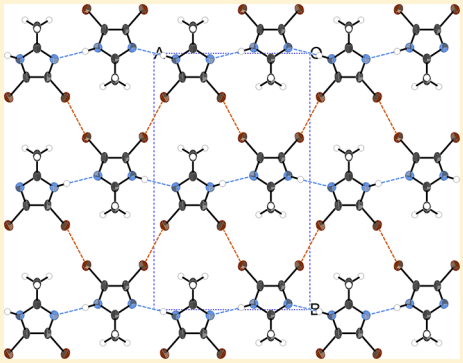

Materials containing switchable bistable hydrogen bonds are of current interest for their potential ferroelectric and relaxor properties: ordering of hydrogen-bonded chains can result in permanent dipole moments (either in the bulk or in nanodomains), which may then be reversed under an externally applied electric field. Although most reported ferroelectric materials are inorganics, simple organic N−H···N hydrogen-bonded materials, such as monoprotonated 1,4-diazabicyclo-[2.2.2]octane[1,2] or imidazole,[3] are now receiving attention. Furthermore, the presence of bistable hydrogen bonds with a low barrier to proton transfer can give rise to proton conductivity, for which imidazole is also of noted interest.[4] However, in order to maintain a continuous current, reorganization of individual molecules must occur, against which there is a high energetic penalty in imidazole itself.[5] Both ferroelectricity and proton conductivity could be exploited to make smaller, greener, and cheaper electronic devices.

Recent studies have worked to improve proton transfer properties of crystalline imidazole and benzimidazole using either high-pressure[6,7] or cocrystallization[8,9] techniques. Proton transport, molecular rotation, and order−disorder transitions could be also addressed through chemical modification, and hence the crystal structures of small functionalized imidazoles that may display altered packing are of interest in this field.

Very recently, imidazolium salts substituted on the ring with a halogen have come to the fore as a major halogen-bonding (XB) motif[10−14] due to the large covalent contribution[15] and overall positive charge. However, the inductive and mesomeric electron-withdrawing effect of the nitrogen atoms in neutral imidazole compounds may also permit a degree of halogen bonding, and therefore, it is possible that the packing of nonquaternized halo-imidazole crystals could be influenced in new ways by halogen-bonding interactions. Furthermore, any halogen bonding observed in neutral imidazole derivatives could serve to facilitate the design of new XB motifs, a field that is sparsely populated compared with the number of established hydrogen-bonding units available to supramolecular chemists.

We present herein crystal structures of methyl- and bromoimidazole derivatives with different substitution patterns and assess the intermolecular forces displayed therein. We also discuss the effect of replacing the electron-donating methyl groups with electron-withdrawing nitrile functionalities and the resulting increase in polarization of the halogen atom.

EXPERIMENTAL PROCEDURES

Synthesis. The syntheses of 4,5-dimethyl-, 2-bromo-4,5-dimethyl-, and 4,5-dibromo-2-methylimidazole have been reported previously.[15] ^{1}H and ^{13}C NMR spectra were recorded on a Varian Mercury VX300 spectrometer. Mass spectrometry was performed on a Bruker microTOF (ESI) spectrometer.

2-Bromo-4,5-dicyanoimidazole.[16] 4,5-Dicyanoimidazole (1.00 g, 8.47 mmol) was added to 1 M NaOH (aq) (25 mL) and stirred until complete dissolution had been achieved. Elemental bromine (1.5 mL, 29.6 mmol) was added carefully, and the resultant mixture was stirred under a nitrogen atmosphere overnight, producing a voluminous white precipitate. The mixture was extracted with ethyl acetate (3 × 25 mL), which was dried over $MgSO_4$, and filtered, giving 2-bromo-4,5-dicyanoimidazole as a white crystalline solid upon solvent removal (1.42 g, 85%). ^{1}H NMR (300 MHz, DMSO-d_6) δ (ppm) no peaks; ^{13}C NMR (125 MHz, DMSO-d_6) δ (ppm) 126.7, 118.4, 112.1; ESMS m/z calcd for $[M + H]^+$ 196.9, found 197.1; mp 84 °C.

N-Benzyl-2-bromo-4,5-dicyanoimidazole. Benzyl bromide (0.97 g, 5.70 mmol), 2-bromo-4,5-dicyanoimidazole (1.02 g, 5.17 mmol), and K_2CO_3 (7.16 g, 51.7 mmol) were stirred overnight in DMF (50 mL) at

Received: February 17, 2013
Revised: May 20, 2013

   dx.doi.org/10.1021/cg400273p | Cryst. Growth Des. XXXX, XXX, XXX−XXX

Table 1. Selected Crystallographic Data for Structures Discussed Herein

Compound	4,5-Dimethyl-imidazole	2-Methyl-imidazole	2-Bromo-4,5-dimethylimidazole	4,5-Dibromo-2-methylimidazole	2-Bromo-4,5-dicyanoimidazole	*N*-Benzyl-2-bromo-4,5-dicyanoimidazole
					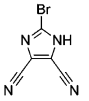	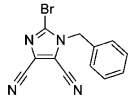
Chemical formula	$C_5H_8N_2$	$C_4H_6N_2$	$C_5H_7Br_1N_2$	$C_4H_4Br_2N_2$	$C_5HBrN_4{\cdot}2(H_2O)$	$C_{12}H_7Br_1N_4$
Crystal system	Monoclinic	Orthorhombic	Orthorhombic	Orthorhombic	Monoclinic	Orthorhombic
a/Å	13.4717(8)	6.0659(4)	3.9495(2)	10.0598(11)	9.5726(5)	16.8783(3)
b/Å	19.3539(11)	8.1508(5)	15.8764(7)	16.5717(19)	8.6753(4)	8.31630(10)
c/Å	6.6371(4)	9.6963(6)	10.1544(4)	4.0208(4)	10.6814(6)	16.7655(3)
α/°	90	90	90	90	90	90
β/°	95.599(3)	90	90	90	104.937(2)	90
γ/°	90	90	90	90	90	90
Unit cell volume/Å^3	1722.24(18)	479.40(5)	636.72(5)	670.30(13)	857.06(8)	2353.29(7)
Space group	$P2_1/c$	$P2_12_12_1$	*Pbcm*	*Ama*2	*C*2/*c*	$Pca2_1$
R_{int}	0.158	0.045	0.020	0.129	0.017	0.066
Final R_1 values ($I > 2\sigma(I)$)	0.0677	0.0457	0.0382	0.0511	0.0310	0.0358
Final $wR(F^2)$ values (all data)	0.1832	0.1339	0.1046	0.1286	0.2463	0.1041

room temperature. After filtration and washing of the solids with acetone (10 mL), the solvent was removed *in vacuo*, leaving the crude product. Purification was achieved by addition of CH_2Cl_2 (50 mL) and subsequent washing with water (3 × 50 mL), followed by drying over $MgSO_4$, filtration, and solvent removal, giving the product as a white crystalline solid (0.51 g, 34%). ^{1}H NMR (200 MHz, $CDCl_3$) δ (ppm) 7.30−7.14 (5H, m, Ar*H*), 5.19 (2H, s, CH_2); ^{13}C NMR (125 MHz, $CDCl_3$) δ (ppm) 132.1, 129.6, 129.5, 127.8, 126.4, 123.5, 114.5, 110.6, 107.4, 52.2; HR-ESMS *m*/*z* calcd for $[M + Na]^+$ 308.9746, found 308.9744; mp 76 °C.

Crystallography. Crystals were obtained in each case by slow evaporation of organic solvents, as specified in the main text (see Table 1). Single-crystal diffraction data were collected using a Nonius Kappa CCD equipped with a Cryostream N_2 open-flow cooling device[17] operating at 150(2) K using graphite monochromated Mo Kα radiation (λ = 0.71073 Å). Series of ω-scans were performed in such a way as to collect every independent reflection to a maximum resolution of 0.77 Å, aiming for 99.5% completeness. Cell parameters and intensity data (including interframe scaling) were processed with DENZO-SMN.[18] Structures were solved with SIR92[19] or SuperFlip[20] and refined using the CRYSTALS package.[21−23] All non-hydrogen atoms were refined with anisotropic displacement parameters. The H atoms were usually visible in the difference map, but those attached to carbon atoms were repositioned geometrically. Protic H atoms that could not be located in the difference map were positioned to satisfy hydrogen-bonding requirements. The H atoms were initially refined with soft restraints on the bond lengths and angles to regularize their geometry (C−H in the range of 0.93−0.98 Å, N−H in the range of 0.86−0.89 Å, and O−H = 0.82 Å, and isotropic displacement factors in the range of 1.2−1.5 times U_{eq} of the parent atom), after which the positions were refined with riding constraints.

RESULTS AND DISCUSSION

Bromo- and Methylimidazoles. The primary packing motif in imidazole-based crystals consists of N−H···N hydrogen-bonded chains of heterocycles, with adjacent molecules oriented in an approximately antiparallel arrangement (Figure 1). Such a structure permits an extended network of linear N−H···N hydrogen bonds with a good degree of close-packing. However, depending upon the substitution pattern of the heterocycle, the hydrogen-bonding distances (and hence proton transfer barriers) and geometry of the chains may be significantly affected by additional interactions, which are the features of note in this study.

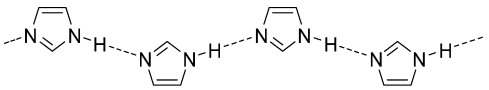

Figure 1. Archetypal hydrogen-bonded packing of imidazoles into chains.

In the reports of the crystal structure of imidazole itself[24−28] (Figure 2), adjacent molecules in the chains are rotated by approximately 120° with respect to each other along the axis of the hydrogen-bonded chain, a distortion that permits the approach of the relatively electron-poor C2 proton to the nitrogen lone pair, thus linking the 1D chains into 2D layers (Figure 2): this can be considered an optimization of the archetypal chain motif that provides an additional electrostatic interaction. The rotation of molecules dominates over π-stacked dispersion interactions, which would be possible in a

dx.doi.org/10.1021/cg400273p | Cryst. Growth Des. XXXX, XXX, XXX−XXX

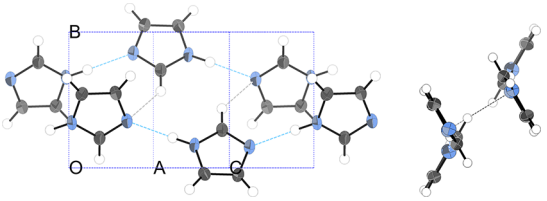

Figure 2. X-ray crystal structure of imidazole (CCDC code IMAZOL03) showing (left) strong N−H (blue) and polar C−H···N (gray) contact, and (right) rotation of imidazole molecules within N−H···H bonded chains. Thermal ellipsoids shown at 50% probability.

purely planar array due to the electron-rich nature of the heterocycle. The reported N(H)···N distance generally varies between 2.842 and 2.869 Å.

Unexpectedly, 4,5-dimethylimidazole crystallized from diethyl ether with three molecules in the asymmetric unit (we have previously reported this structure,[15] but without analysis) (Figure 3); it can be seen that the steric demands of the methyl

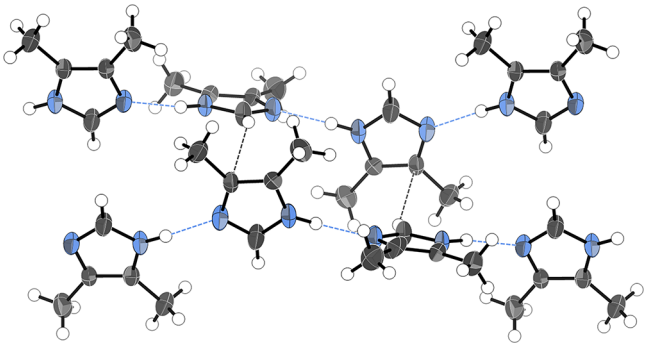

Figure 3. X-ray crystal structure of 4,5-dimethylimidazole, showing hydrogen bonds (blue) and C−H···π interactions (gray). Thermal ellipsoids shown at 50% probability.

groups interfere with the optimal close-packing pattern for unsubstituted imidazole, although the hydrogen-bonded chain is preserved. In this case, two of the molecules are mutually antiparallel (173.5° rotation between the two rings), but the third is distinctly out of plane (rotated by 72.7° and 67.8° compared to the adjacent imidazoles), and takes part in an interchain C−H···π interaction, electrostatically driven by the electron-rich nature of the ring compared to the protons. Overall, each hydrogen-bonded chain has become helical, with both hands being represented in the extended structure due to the centrosymmetric space group ($P2_1/c$). The variety of orientations in this structure suggests that molecular reorganization may have a lower energetic barrier than in imidazole itself, an observation consistent with the lower density (1.112 compared with 1.287 g mL^{-1}). At 2.822(5), 2.834(5), and 2.861(5) Å, the N(H)···N distances include two significantly shorter than those in imidazole itself, indicating a reduced barrier to proton transfer. 4,5-Dimethylimidazole is, therefore, an interesting candidate for future proton conductivity studies.

The structure of 2-methylimidazole has been reported once,[29] but was measured again in this study (Figure 4). Again, hydrogen-bonded chains were observed, but in this case, the hydrogen-bond-linked imidazoles are rotated 168° with respect to each other. The C5 proton approaches the center of a nearby imidazole ring, in a C−H···π contact likely to be driven by electrostatic differences between the δ^+ proton and

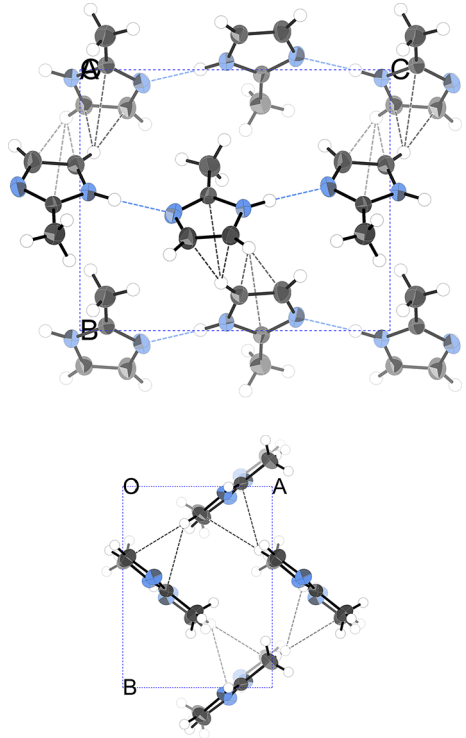

Figure 4. X-ray crystal structure of 2-methylimidazole showing (top) hydrogen bonds (blue) and C−H···π interactions (gray), and (bottom) formation of a tetrad of hydrogen-bonded chains by C−H···π interactions. Thermal ellipsoids shown at 50% probability.

the δ^- π system. Again, a short N(H)···N distance is observed (2.824(4) Å).

Thus, we can see that, in imidazole itself, and *C*-substituted methyl derivatives, the N−H···N hydrogen-bonded chains are supplemented by C−H···π interactions over and above π−π stacking, which would be permitted in alternative packing arrangements with the rings coplanar. A survey of simple imidazole compounds in the Cambridge Structural Database (CSD) found no examples of π−π stacked rings, indicating that comparatively strong electrostatic attractions between the δ^+ protons and the electron-rich π surface outweigh π−π stacking, which only arises primarily due to weak dispersion forces.

In both 2-bromo-4,5-dimethylimidazole and 4,5-dibromo-2-methylimidazole, the location of the N−H proton could not be determined, the two sides of the imidazole being crystallographically indistinguishable, even with respect to bond lengths within the ring. It is likely that the donor−acceptor polarity of the hydrogen-bonded chains varies throughout the crystal, resulting in nano- or microdomains, which may indicate ferroelectric or relaxor properties. The mildly electron-withdrawing effect of the bromine atoms may be responsible for the disorder by increasing the acid−base self-dissociation constant.

The crystal structure of 2-bromo-4,5-dimethylimidazole, grown from chloroform (Figure 5), displayed the greatest similarity to the classical hydrogen-bonded chains, exhibiting no other close contacts. In this case, the N(H)···N distance is long at 2.920(5) Å, presumably due to the increased steric bulk, indicating a higher kinetic barrier to proton transfer than in imidazole.The size of the bromine atom appears to be complementary to the steric demands of the two methyl groups, allowing an almost perfectly antiparallel arrangement, the angle between the planes of adjacent imidazole rings being

dx.doi.org/10.1021/cg400273p | *Cryst. Growth Des.* XXXX, XXX, XXX−XXX

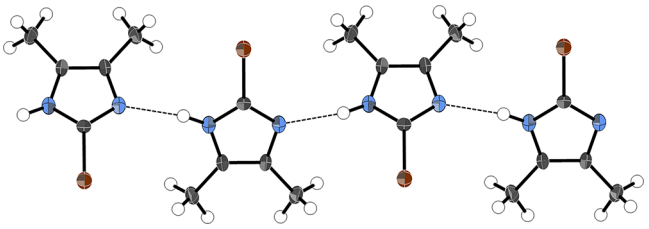

Figure 5. X-ray crystal structure of 2-bromo-4,5-dimethylimidazole. Proton disorder omitted for clarity. Thermal ellipsoids shown at 50% probability.

just 25.3°. This structure highlights the cause of the reduction in symmetry in 4,5-dimethylimidazole: without the bromine, the steric demands of the methyl groups on adjacent-but-one units cause a clash that is resolved by the emergence of helicity.

In 4,5-dibromo-2-methylimidazole (Figure 6), a long N-(H)···N distance is again observed (2.916(11) Å), suggesting a

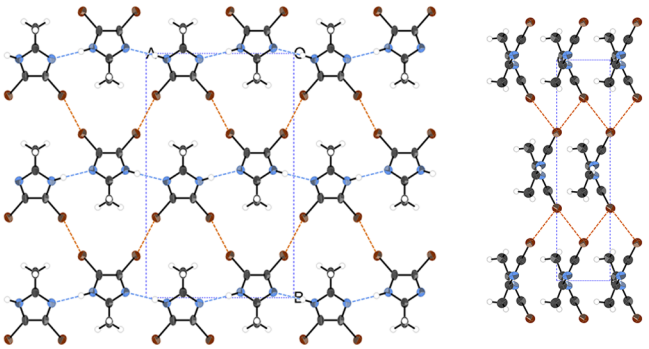

Figure 6. X-ray crystal structure of 4,5-dibromo-2-methylimidazole showing (left) hydrogen bonds (blue) and Br···Br interactions (brown), and (right) side view of Br···Br interactions. Thermal ellipsoids shown at 50% probability.

comparatively high kinetic barrier to proton transfer, while the disorder also indicates the presence of polarity domains.

While no Br···Br contacts were seen in 2-bromo-4,5-dimethylimidazole, by contrast, in 4,5-dibromo-2-methylimidazole, each bromine atom has close contacts (3.552(4) Å, R_{BrBr} = 0.96[30]) with two others, one almost linear (162.5(15)°), and another that is bent (122.7(17)°). The geometry implies that this is due to the difference in charge between the δ^+ tip of the halogen (the σ hole[31]), and the δ^- belt around its meridian, leading to formation of weak halogen bonds in which each bromine atom acts both as a donor and as an acceptor. Presumably, the interaction is facilitated by a combination of the electronic effects of the ring substituents, and the geometric factors that give rise to this packing pattern. Although such amphiphilic halogen bonding has rarely been discussed for bromine[32] (as opposed to iodine[33,34]), a search of the Cambridge Structural Database for sub-van der Waals C−Br···Br−C contacts with angles of 90° and 180° (±10°) gave 227 hits. This figure represents more than half of the 410 results returned without specifying the angles, indicating that these interactions are frequently overlooked.

Despite the preservation of the primary supramolecular motif (the hydrogen-bonded donor−acceptor chain of hermaphroditic imidazole molecules), these structures display a great variety among them. CH−π interactions are observed, as well as simultaneous donor/acceptor halogen bonding. Interestingly, no conventional face-to-face π−π contacts are seen. Although adding methyl groups alone can reduce N(H)···N distances, which may improve proton conductivity, attachment of bromines results in disorder, which may indicate ferroelectric properties.

2-Bromo-4,5-dicyanoimidazoles. To assess the effect of the polarization of the bromine atom in these neutral imidazoles, the methyl groups were replaced with strongly electron-withdrawing cyano groups (Scheme 1). 4,5-Dicyanoimidazole was treated with elemental bromine and aqueous sodium hydroxide to give the 2-bromo derivative in 85% yield. Since haloimidazolium salts are of current interest, we also attempted the stepwise *N*-alkylation, successfully at first, using potassium carbonate and benzyl bromide in DMF, giving *N*-benzyl-2-bromo-4,5-dicyanoimidazole. However, the second *N*-benzylation could not be achieved even under forcing conditions, such as a pressurized microwave reactor with benzyl bromide acting as the solvent, presumably due to the electron-poor nature of the ring depleting the nucleophilicity of the nitrogen atom.

Scheme 1. Synthesis of 2-Bromo-4,5-dicyanoimidazoles

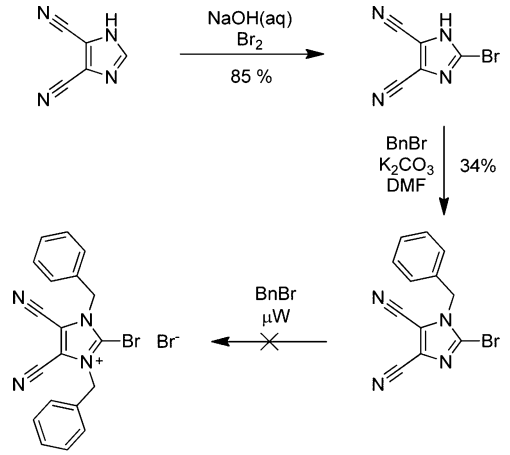

Despite the difficulty in obtaining positively charged 4,5-dicyano-2-halo-imidazolium compounds, given the results discussed above, it appeared likely that the neutral heterocycle could be sufficiently electron-withdrawing to induce a σ hole on the polarizable halogen, and thus provide a new uncharged motif for halogen bond formation. Such interactions have been observed in both 2- and 5-chloro-1-methyl-4-nitroimidazole,[35] which is, in principle, less favorably disposed to halogen bond formation than 2-bromo-4,5-dicyanoimidazole, possessing fewer electron-withdrawing groups and a less polarizable halogen. Single crystals suitable for X-ray diffraction were obtained for 2-bromo-4,5-dicyanoimidazole to examine its hydrogen bonding behavior, and for its *N*-benzyl derivative to provide a second perspective on any halogen-bonding properties.

2-Bromo-4,5-dicyanoimidazole was found to crystallize from evaporating acetone with two molecules of water per molecule (Figure 7). Strong hydrogen bonds enforced the crystal packing, with both nitrogen atoms and water molecules acting as donors and acceptors. While the O−H···N(nitrile) hydrogen bonds were always present, the location of the protons involved in hydrogen bonding with the heterocycle core displayed long-range disorder. As with the bromomethylimidazoliums discussed above, it is likely that nano- or microdomains of donor−acceptor polarity are formed. Although the bromine

dx.doi.org/10.1021/cg400273p | *Cryst. Growth Des.* XXXX, XXX, XXX−XXX

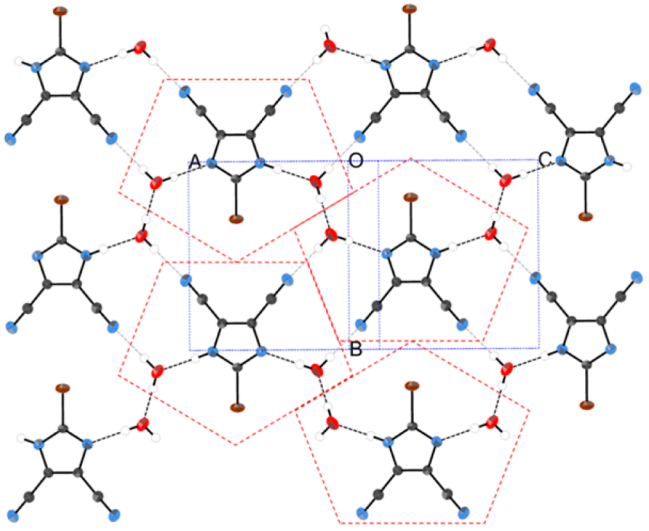

Figure 7. X-ray crystal structure of 2-bromo-4,5-dicyanoimidazole·$2H_2O$, showing disordered (black) and ordered (gray) hydrogen bonds. Pentagonal supramolecules indicated with dotted red lines. Thermal ellipsoids shown at 50% probability.

atom is directed toward an electron-rich end of an adjacent molecule (i.e., dipoles are aligned), no halogen short contacts occur.

Interestingly, if the two water molecules hydrogen-bonded through the ring nitrogen atoms are considered as part of a single supramolecular entity with the heterocycle, forming a pseudo-5-fold symmetric tile (indicated by the dashed red lines), the arrangement constitutes the optimal 2D close-packing for regular pentagons, which has only recently been reported in a highly engineered crystal structure.[36] More intriguingly in this case, the inclusion of water from an (undried) organic solvent means that the packed pentagonal structure has been favored spontaneously by a strong thermodynamic driving force here, rather by human design.

The crystal structure of *N*-benzyl-2-bromo-4,5-dicyanoimidazole (Figure 8), containing two molecules in the asymmetric unit, displayed a number of interesting features. While no classical halogen bonding was observed, close contacts (3.365(4) and 3.317(4) Å, R_{BrC} = 0.95, 0.93) were observed between the bromine atoms and the π system of the benzene ring, with nearly linear geometry (165.68(15) and 162.00(16)°) to an aryl carbon atom (exactly 180° would put the point of contact closer to the centroid of the ring). This is consistent with the delocalized aromatic electron density acting as a halogen bond acceptor, analogous to the complex of benzene and dibromine with a C···Br distance of 3.18 Å.[37] Such halogen-bonding contacts with π systems have also been documented with the C≡N bonds of cyanide ligands attached to metal centers,[38,39] and to the π systems of aryl ligands for metals,[40] and are perhaps more common still.[41] Furthermore, significant lone pair−π interactions are seen between the imidazole nitrogen and the electron-deficient carbons of the nitrile groups on an adjacent molecule (3.073(5), 3.128(5), 3.072(5), 3.244(5) Å; R_{CN} = 0.95−0.99). The Lewis basic nitrogen bridges the dicyano system, sitting almost equidistant from each carbon. The intermolecular forces at play in this crystal serve, therefore, to highlight the variety of intermolecular interactions that can occur using simple molecules, and have yet to be employed in the strategic fabrication of self-assembled supramolecular constructs.

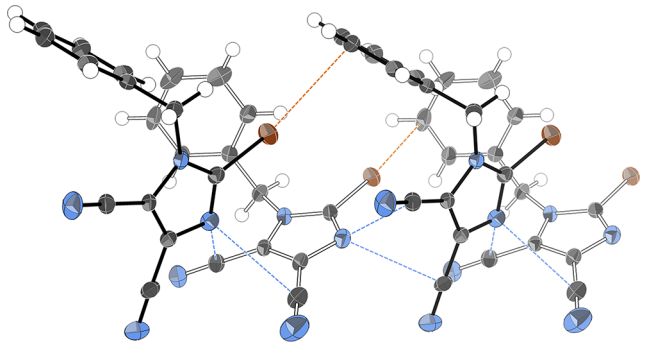

Figure 8. X-ray crystal structure of *N*-benzyl-2-bromo-4,5-dicyanoimidazole showing nonclassical halogen bonds (brown) and N−C interactions (blue). The black- and white-bonded molecules are not symmetry-related. Thermal ellipsoids shown at 50% probability.

CONCLUSIONS

We have reported six new crystal structures of imidazole derivatives, which display a variety of intermolecular interactions. From a fundamentals perspective, the (albeit weak) halogen bonds formed despite the lack of quaternization (i.e., positive charge on the heterocycle) are of particular note: amphiphilic Br···Br halogen bonds in the case of 4,5-dibromo-2-methylimidazole and Br···π in *N*-benzyl-2-bromo-4,5-dicyanoimidazole. Such interactions could be used for further crystal engineering applications, or taken beyond into broader supramolecular assembly and host−guest chemistry. Viewed through the lens of proton-transfer materials, the shorter N(H)···N distances combined with lower densities in methylimidazoles are of interest for proton conduction studies, whereas the disorder seen in the bromo derivatives may result in interesting ferroelectric and relaxor properties.

ASSOCIATED CONTENT

Supporting Information

Crystal structures in CIF format. This material is available free of charge via the Internet at http://pubs.acs.org.

AUTHOR INFORMATION

Corresponding Author

*E-mail: christopher.serpell@mcgill.ca.

Present Address

†Department of Chemistry, McGill University, Room 400, 801 Sherbrooke St. West, Montreal, Quebec, H3A 0B8, Canada.

Author Contributions

All authors have given approval to the final version of the manuscript.

Notes

The authors declare no competing financial interest.

ACKNOWLEDGMENTS

We thank Oxford University Chemical Crystallography for use of the instruments, and Amber L. Thompson for technical expertise and comments on this manuscript. C.J.S. thanks Johnson Matthey and the EPSRC for a CASE studentship and the EPSRC for a PhD+ award.

REFERENCES

(1) Katrusiak, A.; Szafrański, M. *Phys. Rev. Lett.* **1999**, *82*, 576.

(2) Szafrański, M.; Katrusiak, A. *J. Phys. Chem. B* **2004**, *108*, 15709.
(3) Katrusiak, A. *J. Mol. Struct.* **1999**, *474*, 125.
(4) Kawada, A.; McGhie, A. R.; Labes, M. M. *J. Chem. Phys.* **1970**, *52*, 3121.
(5) Daycock, J. T.; Jones, G. P.; Evans, J. R. N.; Thomas, J. M. *Nature* **1968**, *218*, 672.
(6) Paliwoda, D.; Dziubek, K. F.; Katrusiak, A. *Cryst. Growth Des.* **2012**, *12*, 4302.
(7) Zieliński, W.; Katrusiak, A. *Cryst. Growth Des.* **2013**, *13*, 696.
(8) Ławniczak, P.; Pogorzelec-Glaser, K.; Cz, P.; Pietraszko, A.; Szcześniak, L. *J. Phys.: Condens. Matter* **2009**, *21*, 345403.
(9) Pogorzelec-Glaser, K.; Rachocki, A.; Lawniczak, P.; Pietraszko, A.; Pawlaczyk, C.; Hilczer, B.; Pugaczowa-Michalska, M. *CrystEngComm* **2013**, *15*, 1950.
(10) Walter, S. M.; Kniep, F.; Herdtweck, E.; Huber, S. M. *Angew. Chem., Int. Ed.* **2011**, *50*, 7187.
(11) Cametti, M.; Raatikainen, K.; Metrangolo, P.; Pilati, T.; Terraneo, G.; Resnati, G. *Org. Biomol. Chem.* **2012**, *10*, 1329.
(12) Caballero, A.; White, N. G.; Beer, P. D. *Angew. Chem., Int. Ed.* **2011**, *50*, 1845.
(13) Caballero, A.; Zapata, F.; White, N. G.; Costa, P. J.; Félix, V.; Beer, P. D. *Angew. Chem., Int. Ed.* **2012**, *51*, 1876.
(14) Walter, S. M.; Kniep, F.; Rout, L.; Schmidtchen, F. P.; Herdtweck, E.; Huber, S. M. *J. Am. Chem. Soc.* **2012**, *134*, 8507.
(15) Serpell, C. J.; Kilah, N. L.; Costa, P. J.; Félix, V.; Beer, P. D. *Angew. Chem., Int. Ed.* **2010**, *49*, 5322.
(16) Apen, P. G.; Rasmussen, P. G. *Heterocycles* **1989**, *29*, 1325.
(17) Cosier, J.; Glazer, A. M. *J. Appl. Crystallogr.* **1986**, *19*, 105.
(18) Otwinowski, Z.; Minor, W. *Processing of X-ray Diffraction Data Collected in Oscillation Mode*; Methods in Enzymology; Academic Press: New York, 1997; Vol. *276*.
(19) Altomare, A.; Cascarano, G.; Giacovazzo, C.; Guagliardi, A.; Burla, M. C.; Polidori, G.; Camalli, M. *J. Appl. Crystallogr.* **1994**, *27*, 435.
(20) Palatinus, L.; Chapuis, G. *J. Appl. Crystallogr.* **1997**, *40*, 786.
(21) Betteridge, P. W.; Carruthers, J. R.; Cooper, R. I.; Prout, K.; Watkin, D. J. *J. Appl. Crystallogr.* **2003**, *36*, 1487.
(22) Cooper, R. I.; Thompson, A. L.; Watkin, D. J. *J. Appl. Crystallogr.* **2010**, *43*, 1100.
(23) Thompson, A. L.; Watkin, D. J. *J. Appl. Crystallogr.* **2011**, *44*, 1017.
(24) Martinez-Carrera, S. *Acta Crystallogr.* **1966**, *20*, 783.
(25) Will, G. *Z. Kristallogr., Kristallgeom., Kristallphys., Kristallchem.* **1969**, *129*, 211.
(26) Omel'chenko, Y. A.; Kondrashev, Y. D. *Kristallografiya (Russ.)* **1971**, *16*, 115.
(27) Craven, B. M.; McMullan, R. K.; Bell, J. D.; Freeman, H. C. *Acta Crystallogr., Sect. B: Struct. Crystallogr. Cryst. Chem.* **1977**, *33*, 2585.
(28) McMullan, R. K.; Epstein, J.; Ruble, J. R.; Craven, B. M. *Acta Crystallogr., Sect. B: Struct. Crystallogr. Cryst. Chem.* **1979**, *35*, 688.
(29) Hachuła, B.; Nowak, M.; Kusz, J. *J. Chem. Crystallogr.* **2010**, *40*, 201.
(30) Normalized distances $R_{XY} = d(XY)/(r_X + r_Y)$, where r_X and r_Y refer to van der Waals radii.
(31) Clark, T.; Hennemann, M.; Murray, J.; Politzer, P. *J. Mol. Model.* **2007**, *13*, 291.
(32) Assouma, C. D.; Crochet, A.; Chérémond, Y.; Giese, B.; Fromm, K. M. *Angew. Chem., Int. Ed.* **2013**, *52*, 4682.
(33) Reddy, C. M.; Kirchner, M. T.; Gundakaram, R. C.; Padmanabhan, K. A.; Desiraju, G. R. *Chem.—Eur. J.* **2006**, *12*, 2222.
(34) Olejniczak, A.; Katrusiak, A.; Vij, A. *CrystEngComm* **2009**, *11*, 1073.
(35) Kubicki, M.; Wagner, P. *Acta Crystallogr.* **2007**, *C63*, o454.
(36) Ren, C.; Zhou, F.; Qin, B.; Ye, R.; Shen, S.; Su, H.; Zeng, H. *Angew. Chem., Int. Ed.* **2011**, *50*, 10612.
(37) Rosokha, S. V.; Kochi, J. K. In *Halogen Bonding: Fundamentals and Applications*; Metrangolo, P., Resnati, G., Eds.; Springer: Berlin, 2008; Vol. *126*.
(38) Derossi, S.; Brammer, L.; Hunter, C. A.; Ward, M. D. *Inorg. Chem.* **2009**, *48*, 1666.
(39) Ormond-Prout, J. E.; Smart, P.; Brammer, L. *Cryst. Growth Des.* **2011**, *12*, 205.
(40) Lapadula, G.; Judaš, N.; Friščić, T.; Jones, W. *Chem.—Eur. J.* **2010**, *16*, 7400.
(41) Gamez, P. *CrystEngComm* **2013**, *15*, 1802.